Dear Editor,

Thank you very much for your handling our manuscript "**Mechanistic insights into marine boundary layer nucleation: synergistic interactions of typical sulfur, iodine, and nitrogen precursors**" (MS No.: egusphere-2025-5622). According to reviewer's valuable and helpful comments, we have revised the manuscript carefully and listed the point-to-point responses to the reviewers' comments as below:

Referee #1:

Jing Li and colleagues investigated the synergistic nucleation mechanism involving typical sulfur-, iodine-, and nitrogen-containing chemical species in marine regions—specifically, methanesulfonic acid (MSA), iodic acid (IA), and dimethylamine (DMA)—in a process referred to as the IA–MSA–DMA ternary nucleation mechanism. This study systematically examines the IA–MSA–DMA ternary nucleation system, addressing cluster stability, thermodynamic and kinetic properties, and the molecular-level mechanisms involved. The findings highlight the importance of synergistic nucleation among sulfur, iodine, and nitrogen compounds, offering deeper insight into marine secondary aerosol formation, particularly given the chemical complexity of the real atmosphere. This is a clearly written manuscript on a topic of high atmospheric relevance. The proposed mechanism, once implemented in atmospheric models, is likely to sharpen simulations of aerosol formation and associated climate responses. I am therefore inclined to recommend publication in *Atmospheric Chemistry and Physics*, subject to consideration of the minor points listed below, which mainly concern the interpretation of the theoretical results.

Response: We sincerely thank the reviewer for the careful and professional assessment of our manuscript. We have revised the manuscript accordingly, with detailed point-by-point responses provided below.

---

1. The nucleation process typically entails a competition between cluster collision and

evaporation. It would be helpful if the authors could specify which specific types of these processes were included in their ACDC simulations. We recommend adding these details to the ACDC methodology section for clarity.

Response: We appreciate the reviewer's insightful comment. The professional comment is beneficial in enhancing the readers' understanding of more simulation details. Accordingly, the detailed settings about the collision and evaporation processes in ACDC simulations have been added in the revised manuscript (lines 94-96, page 4) as follows:

"*In this study, the conducted ACDC simulations accounted for all feasible collision and evaporation processes. These included interactions between monomer-monomer, monomer-cluster, and cluster-cluster pairs, in addition to the fragmentation of parent clusters into monomers or into two smaller clusters.*"

---

2. It is worth noting that iodous acid typically co-occurs with iodic acid in marine environments as a homologous species. While the authors have compared their work with the iodic acid-iodous acid system, the influence of iodous acid itself was not considered in this study. To better isolate the variables and make the comparison more accurate, it might be beneficial to simultaneously account for the effect of MSA as well. In addition, in a previous study (*Atmos. Chem. Phys*., 2024, 24, 3989), the authors have already investigated the MSA–HIO_3–HIO_2 system. I would therefore recommend not only comparing with the HIO_3–HIO_2 system, but also making a more direct comparison with the MSA–HIO_3–HIO_2 system. This would be a meaningful extension and would more clearly highlight the synergistic roles of multiple components.

Response: Thanks for the reviewer's insightful suggestion. As the reviewer rightly points out, the influence of iodous acid (HIO_2) was not considered in this work. Indeed, our results should have been compared with those from the previous study on the MSA–HIO_3–HIO_2 system, as such a comparison would better highlight the significance of the IA–MSA–DMA system. Consequently, we have further compared the rates of the two systems. As shown in Fig. S4, the nucleation rate of the IA–MSA–DMA system can be up to two orders of magnitude higher than

that of the MSA–HIO_3–HIO_2 system under comparable conditions. This comparison has been included and discussed in the revised manuscript (lines 217-221, page 9), as follows:

"*Furthermore, we compared the nucleation rates of the IA–MSA–DMA system with those of the IA–MSA–HIO_2 system. The results indicate that the inclusion of DMA as a strong base in the ternary system markedly enhances cluster formation. Specifically, across the studied temperature and concentration ranges, the calculated nucleation rate for the IA–MSA–DMA mechanism exceeds that of the IA–MSA–HIO_2 system by up to two orders of magnitude (Fig. S4).*"

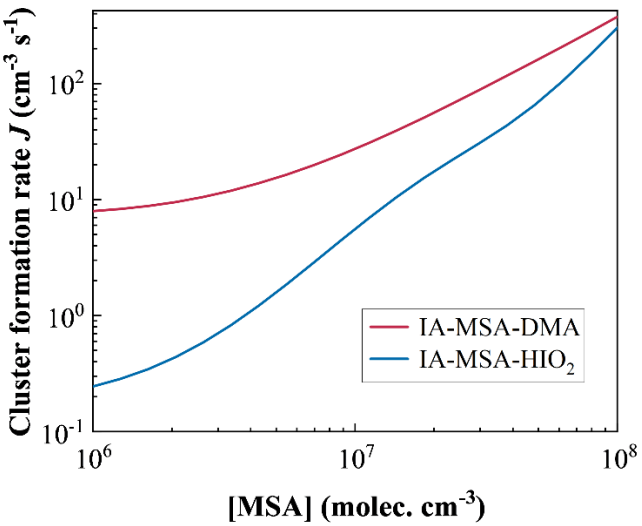

Figure S4. Cluster formation rates J (cm^{-3} s^{-1}) of the IA–MSA–DMA and IA–MSA–HIO_2 systems under conditions of T = 278 K, CS = 2.0×10^{-3} s^{-1}, [IA] = 10^7 molec. cm^{-3}, [MSA] = $10^6 - 10^8$ molec. cm^{-3}, [DMA] = 0.25 pptv, and [HIO_2] = 2.0×10^5 molec. cm^{-3}.

---

3. Computational results can be influenced by various factors, introducing inherent uncertainties. For instance, uncertainties may arise from the quantum chemical calculations and from the cluster dynamic simulations. It would be valuable to include a discussion of these potential uncertainties and their possible impact on the findings.

Response: Thanks for the reviewer's professional and helpful comments. The uncertainties in quantum chemical calculations arise from the resulting Gibbs free energies of cluster formation

($\Delta G = \Delta E + \Delta G_{thermal}$). According to previous studies, the dominant source of uncertainty in free-energy calculations arises from the underlying single-point energy evaluations. We therefore employed the high-level DLPNO-CCSD(T) approach, which has been successfully applied in nucleation studies (Zhang et al., 2022; Ma et al., 2023; He et al., 2023). Systematic benchmark study shows that the DLPNO-CCSD(T) energies agree closely with the gold-standard CCSD(T) results, with a mean absolute deviation of approximately 0.2 kcal mol^{-1} (Liakos et al., 2020). Herein, we examined the uncertainty in cluster formation rates (J, cm^{-3} s^{-1}) stemming from free-energy calculations by varying ΔG by ±0.2 kcal mol^{-1} under marine boundary layer conditions. As shown in Fig. S5(a), perturbing ΔG_{278K} by ±0.2 kcal mol^{-1} results in only minor changes in the J values, within one order of magnitude, under the conditions of T = 278 K, CS = 2.0 × 10^{-3} s^{-1}, [IA] = 10^5 – 10^8 molec. cm^{-3}, [MSA] = 10^7 molec. cm^{-3}, and [DMA] = 0.25 pptv. This indicates that the uncertainty in the quantum chemical calculations do not materially affect the conclusions of this study. In addition, we examined the sensitivity of the nucleation rate J to variations in the collision enhancement factor arising from van der Waals interactions. As shown in Fig. S5(b), changing the sticking factor (SF) from 2.1 to 2.5 results in only minor variations in J, indicating that this effect does not influence the conclusions of the present study.

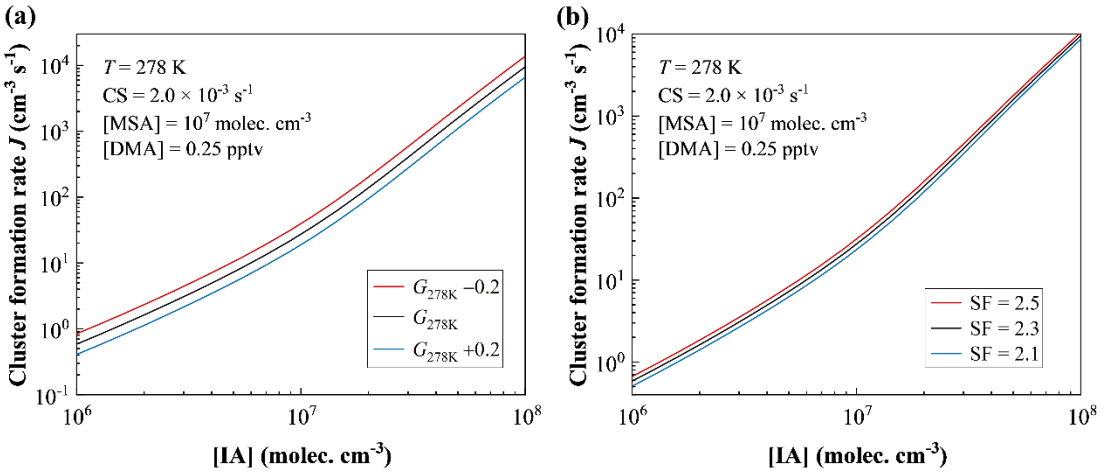

Figure S5. (a) Cluster formation rate J as a function of IA concentration ([IA] = 10^6 – 10^8 molec. cm^{-3}) under different Gibbs free energy values: $\Delta \boldsymbol{G}_{278K}$ (black line), $\Delta \boldsymbol{G}_{278K}$ + 0.2 (blue line), and $\Delta \boldsymbol{G}_{278K}$ – 0.2 (red line). Conditions: $\boldsymbol{T}$ = 278 K, CS = 2.0 × 10^{-3} s^{-1}, [MSA] = 10^7 molec.

cm^{-3}, and [DMA] = 0.25 pptv. **(b)** *J* for the IA–MSA–DMA system under different sticking factor (SF) conditions.

Here, we have added the results of *J* under different Gibbs free energy and sticking factors to the revised Supporting Information, and for the convenience of the review, we have copied Figure S5 and the corresponding analysis (lines 229-232, page 9 in the revised manuscript) as following:

"*Additionally, to account for potential uncertainties in quantum chemical calculations and cluster dynamic simulations, we also examined the effects of the calculated ΔG of clusters and the enhancement factor (sticking factor, SF) on J. As shown in Fig. S5, under boundary-layer conditions, variations in the ΔG (±0.2 kcal* mol^{-1}*) (Liakos et al., 2020) of clusters and the SF (2.1 – 2.5) in dynamic simulations lead to only minor changes in J.*"

---

4. We suggest conducting two sets of calculations representing polluted (CS larger than 0.002/s) and relatively clean conditions, respectively, given that DMA is generally more abundant in polluted environments. This would help establish a more comprehensive understanding of the nucleation mechanism, thereby providing a valuable reference for future research in highly polluted coastal regions.

Response: Following the professional advice of the reviewer, we have performed a more comprehensive simulation of IA–MSA–DMA nucleation under the polluted and relatively clean marine boundary layer (MBL) conditions. As shown in Fig. R1, we compared the IA–MSA–DMA cluster formation rates *J* (cm^{-3} s^{-1}) under clean and polluted conditions. The simulation conditions for the clean environment were $T = 278$ K, CS = 2.0×10^{-3} s^{-1}, [MSA] = 10^7 molec. cm^{-3}, and [DMA] = 0.25 pptv, while for the polluted environment they were $T = 278$ K, CS = 1.0×10^{-2} s^{-1}, [MSA] = 10^7 molec. cm^{-3}, and [DMA] = 2.2 pptv. As [IA] increases, the calculated *J* of IA–MSA–DMA system rise under both clean and polluted MBL conditions. However, the *J* values are consistently higher under polluted MBL conditions than under clean MBL conditions. This is consistent with the conclusions in this study, further validating the

reliability of the present findings.

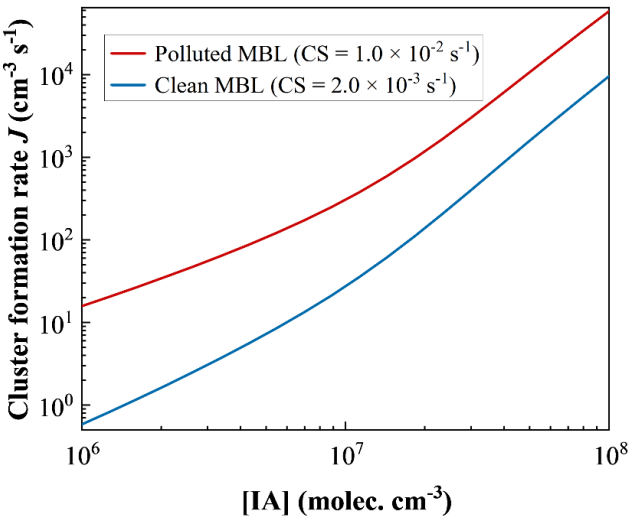

Figure R1. The cluster formation rate J of IA–MSA–DMA system under clean (T = 278 K, CS = 2.0 × 10^{-3} s^{-1}, [MSA] = 10^7 molec. cm^{-3}, and [DMA] = 0.25 pptv) and polluted (T = 278 K, CS = 1.0 × 10^{-2} s^{-1}, [MSA] = 10^7 molec. cm^{-3}, and [DMA] = 2.2 pptv) MBL conditions.

---

5. For the three classes of precursors (sulfur-, iodine-, and nitrogen-containing species), nucleation is jointly driven by their synergistic effects, and the nucleation rate is therefore expected to exhibit different sensitivities to each component. Although the authors have examined the response of the nucleation rate to variations in individual precursor concentrations in Figs. 4d–f, it would be better to also provide a three-dimensional response surface illustrating the joint dependence of the nucleation rate on the simultaneous variation of all three precursor concentrations.

Response: Thanks for the reviewer's helpful comment. Following the reviewer's suggestion, we have plotted a three-dimensional response surface (Fig. S6) to visualize the joint dependence of the nucleation rate on the simultaneous variation of all three precursor concentrations ([IA], [MSA], and [DMA]).

As shown in Figs. S6(b)-(d), when the concentration of any one precursor is held constant, the nucleation rate increases with the concentration of the other two precursors, indicating

significant sensitivity to variations in each component. This result further supports the synergistic role of sulfur-, iodine-, and nitrogen-containing precursors in the nucleation process. Their collective presence enhances the efficiency of new particle formation, and this synergy is clearly reflected in the response of the nucleation rate to changes in the concentration of each precursor class. It can be observed, however, that *J* responds most rapidly to changes in [IA], followed by [DMA], while the response to [MSA] is the slowest. The 3D response surface complements the single-factor sensitivity analysis presented earlier (Figs. 4d–f) and provides a more complete picture of the multi-precursor synergistic nucleation mechanism, thereby strengthening our main conclusion that nucleation is jointly driven by all three types of precursors.

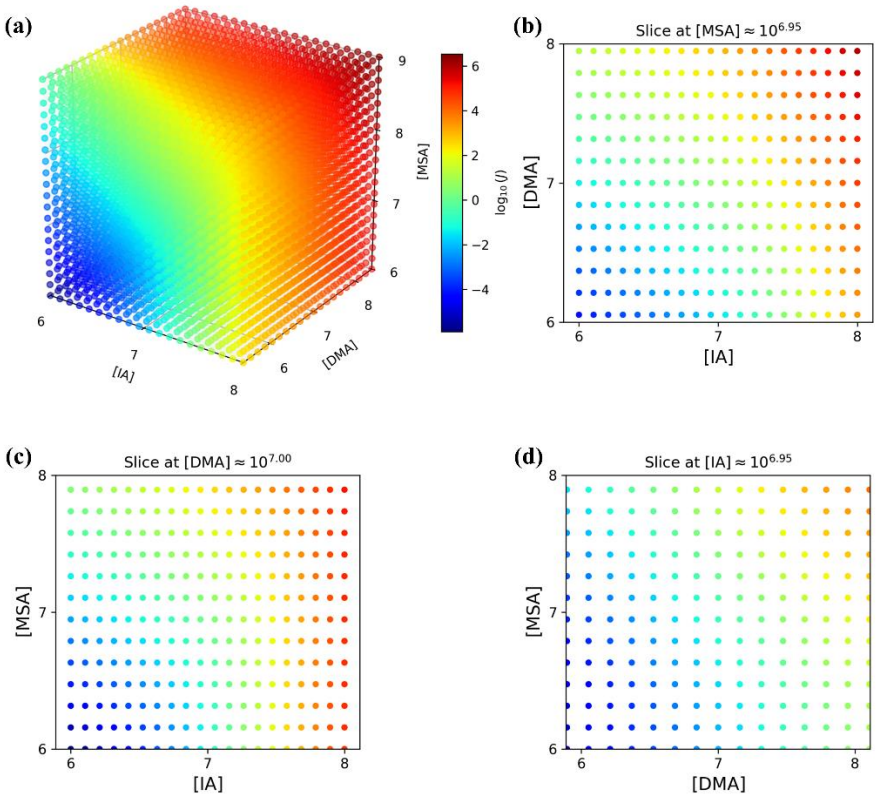

Figure S6. Three-dimensional response surface of the nucleation rate to precursor concentrations. **(a)** Full 3D surface showing the joint dependence on IA, MSA, and DMA. **(b–d)** Two-dimensional projections with one precursor concentration held constant, demonstrating sensitivity to the other two: **(b)** fixed [IA], **(c)** fixed [MSA], and **(d)** fixed [DMA].

We have copied Figure S6 and the corresponding analysis (lines 255-258, page 10 in the

revised manuscript) as following:

"*The three-dimensional response surface also shows that when the concentration of any one precursor is held constant, the J increases with the concentration of the other two precursors, indicating significant sensitivity to variations in each component. However, J responds most rapidly to changes in [IA], followed by [DMA], while the response to [MSA] is the slowest (Fig. S6).*"

---

6. Figure 2: To enhance clarity, please consider adding explicit labels in the figure indicating the meaning of the solid and dashed lines.

Response: We thank the reviewer for the careful comments and have revised Figure 2 accordingly in the revised manuscript.

---

7. For the reader's convenience, please ensure that any abbreviations are written out in full when first introduced, with the abbreviated form following in parentheses. This will allow for the use of the abbreviation alone in subsequent text.

Response: Thanks for the reviewer's helpful suggestion. We have now revised the manuscript to ensure that all abbreviations are spelled out in full at first mention, followed by the abbreviated form in parentheses, as suggested.

Referee #2:

Jing Li and coworkers have investigated the ability of iodic acid (IA), methanesulfonic acid (MSA), and dimethylamine (DMA) to drive nucleation in the troposphere. The binary IA-DMA, MSA-DMA, and IA-MSA clusters are adopted from previous studies, and they have expanded upon this set by looking at the ternary IA-MSA-DMA clusters. These types of more complex systems are important to study given that the atmosphere consists of a wide array of nucleation precursors at varying concentrations at any given point. The paper suggests that the MSA assisted pathway is very efficient and essential for aligning simulated nucleation rates with measured rates at polar sites such as Marambio and Aboa.

This is an interesting study that expands upon our understanding of marine atmospheric nucleation. However, some of the discussion, especially related to the field observations should be reconsidered before publication is advised.

Response: We appreciate the reviewer for dedicating time to assess our manuscript and providing valuable comments and positive feedback.

---

1) Abstract

Lines 10-13: *"Given the coexistence of multiple marine nucleating agents, here we explored how typical sulfur-, iodine-, and nitrogen-bearing chemicals, i.e., methanesulfonic acid (MSA), iodic acid (IA), and dimethylamine (DMA), synergistically interact to drive particle nucleation at the molecular level, by high-level quantum chemical calculations and cluster dynamics simulations."*

This formulation appears a bit odd. Perhaps turn the sentence around or break in two.

Response: Following the reviewer's professional suggestion, we have revised the manuscript by splitting the original sentence into two sentences, as shown below:

"Sulfur-, nitrogen-, and iodine-containing species are expected to coexist in the marine atmosphere, including the canonical precursors methanesulfonic acid (MSA), iodic acid (IA),

and dimethylamine (DMA). To elucidate how they interact to drive NPF, we performed high-level quantum chemical calculations and cluster dynamics simulations to investigate their synergistic nucleation mechanism at the molecular level."

Lines 18-20: *"In polar coastal regions such as Aboa and Marambio, the simulated rates of IA–MSA–DMA nucleation better agree with field measurements compared with the established IA–DMA nucleation."*

I would be careful with the formulation *"better agree with field measurements"* here. As the studied mechanism does not cover all possible nucleators, other species will also contribute. This would effectively push the current results outside the experimental range. Please reformulate.

Response: Thanks. This suggestion is helpful in improving the accuracy of the presentation. We agree with the reviewer that the phrase "*better agree with field measurements*" requires caution. Since our model does not exhaustively include all potential nucleating agents, claiming "better agreement" carries the risk of ignoring other contributors. Here, we have revised the text to clarify that the IA–MSA–DMA system reduces the gap between simulated and observed rates compared to the binary IA–DMA system, suggesting it is likely a significant mechanism rather than the sole explanation. For your convenience, the revisions made in the manuscript are copied below.

"*In polar coastal regions such as Aboa and Marambio, the inclusion of the IA–MSA–DMA nucleation pathway brings simulated nucleation rates closer to field measurements than considering the established IA–DMA nucleation alone, identifying it as a potentially important mechanism in these environments.*"

---

2) Quantum Chemistry Calculations

Spin-orbit coupling: We are missing some specification on how the spin-orbit coupling was calculated. Only a DFT functional/basis set combination is given. The only method for

calculating SOC in Gaussian would be the CASSCF routine. We think that you should expand upon how the SOC was calculated: If CASSCF was applied, what are the orbital spaces / how where they determined?

Response: We thank the reviewer for this important comment regarding the calculation of spin-orbit coupling (SOC). We acknowledge that for systems containing heavy atoms belonging to the fifth period, such as iodine, relativistic effects are significant. These effects comprise both scalar relativistic effects and spin-orbit coupling (SOC). In this study, the scalar relativistic effects have been effectively accounted for by the adopted pseudopotential basis set (aug-cc-pVTZ-PP). And the SOC effects of iodine were represented by the energy difference arising from the inclusion of spin–orbit interactions within the Spin-orbit DFT (SODFT) framework, as implemented in Gaussian 16 using the dhf-TZVP-2c basis set, which includes scalar potential and spin-orbit potential. Here, the effect of SOC on the binding energy of IA-containing clusters is quantified by ΔE_{SOC}, defined as the energy difference between calculations performed with and without SOC potential.

$$\Delta E_{SOC} = E_2 - E_1$$

where E_2 and E_1 represent the single-point energies calculated with and without spin-orbit potential, respectively.

The reviewer correctly notes that a multiconfigurational approach (e.g., CASSCF) is often employed for precise SOC evaluations. The CASSCF method is computationally too expensive to be applicable beyond small systems (Engsvang et al., 2024; Khanniche et al., 2016; Khanniche et al., 2017) and is therefore impractical for atmospheric nucleation clusters, which typically consist of several tens of atoms (e.g., the $(IA)_1(MSA)_2(DMA)_3$ cluster contains 53 atoms).

Notably, the rigorous benchmark study by Engsvang et al. (2024) has demonstrated that SOC-induced energy corrections obtained at the DKH-ωB97X-D3BJ/aug-cc-pVQZ-DK level of theory are below < 0.2 kcal mol^{-1}. And the SOC contributions estimated in the present work fall within the similar range, and in close agreement with these benchmark results. This consistency validates the reliability of our SOC treatment and jointly indicates that spin-orbit

coupling has only a minor energetic impact on iodine-containing clusters. Accordingly, given the small SOC corrections and the high computational cost, the CASSCF-based SOC calculations were therefore not pursued in this study.

Electronic energies: We are missing some discussion on the accuracy of your choice of method for calculating electronic energies. While DLPNO-CCSD(T)/aug-cc-pVTZ or similar has been shown to be quite capable when it comes to lighter elements, it is not necessarily the case for heavier elements. You use aug-cc-pVTZ-PP for iodine, which can at least partially correct for this, however the question is: is it enough? You cite Engsvang 2024, for incorporating SOC, which also touches upon that question. Your choice of method is tested and shown in figure 4b of that study. There, it was found that you should be expecting overbinding of your clusters, and thus too stable clusters, and recommended that you use scalar-relativistic methods for electronic energies. We are not asking you to redo the calculations at another level, but the accuracy/bias of the calculations should be considered when discussing the results.

Response: We appreciate the reviewer's concern regarding the accuracy of electronic energies for heavy elements like iodine. We are aware of the important findings by Engsvang et al. (2024) regarding the potential risk of overbinding when using pseudopotentials (PP) compared to scalar-relativistic Hamiltonians.

Although the reviewer kindly suggested that re-calculation was not mandatory, we felt it was important to quantitatively validate our chosen level of theory to ensure the robustness of our conclusions. Herein, we performed additional single-point energy calculations on the studied iodine-containing clusters using the scalar-relativistic ZORA-CCSD(T)/TZVPP method, which is recommended as the benchmark (Engsvang et al., 2024). Specifically, we calculated single-point energies of the $(IA)_1(DMA)_1$, $(IA)_1(MSA)_1$, and $(IA)_1(DMA)_1(MSA)_1$ clusters at the ZORA-CCSD(T)/TZVPP level of theory. These results were compared with our original DLPNO-CCSD(T)/aug-cc-pVTZ(-PP) results. As summarized in Table R1 below, the difference in electronic energy (ΔE) between the two methods are small (0.17–1.68 kcal mol^{-1}). This confirms that our original method does not suffer from significant overbinding and is

accurate for the systems studied.

Table R1. Comparison of single-point electronic energies (in kcal mol^{-1}) for selected clusters.

Clusters	ΔE (ZORA-CCSD(T))	ΔE (DLPNO-CCSD(T))	$\Delta\Delta E$
$(IA)_1(DMA)_1$	-22.81	-24.49	1.68
$(IA)_1(MSA)_1$	-24.78	-24.95	0.17
$(IA)_1(DMA)_1(MSA)_1$	-52.48	-51.50	0.98

Moreover, the DLPNO-CCSD(T)/aug-cc-pVTZ(-PP) level of theory employed here has been widely adopted in recent studies of iodine-containing atmospheric clusters and has demonstrated good agreement with CLOUD chamber measurements (Ma et al., 2023; He et al., 2023), further supporting its applicability.

---

3) The Cluster Structures

Figure 1: It is not clear what figure 1 and the associated text contributes with. It is essentially showing the definition of intermolecular interactions, which are quite easily seen visually in the figure of the structures in the SI.

Response: We agree that the geometric structures (in the SI) visualize how the molecules interact. However, the electrostatic potential (ESP) maps in Fig. 1 serves a fundamentally different perspective by revealing the electronic structures of the nucleating monomers, thereby providing insight into the intrinsic nature of cluster formation, which cannot be captured by structural diagrams alone. For example, ESP analysis can reveal the halogen-bonding (XB) sites (that is, the σ-hole) of iodine-containing species, which cannot be visualized from molecular geometries. Moreover, comparing ESP values allows a quantitative assessment of the relative strengths of different binding sites, thereby offering quantitative evidence for binding hierarchies and selectivity. In summary, Fig.1 provides the theoretical rationale and

visual evidence for why and where the specific intermolecular interactions (hydrogen bonds (HBs) and XBs) discussed in our manuscript are expected to occur.

Lines 135-136, and 306: You comment on the proportion of bonds which are hydrogen bonds (HBs). It is concluded that HBs are dominant because they make up 74%. It is unclear how you arrive at this number. Is it the number of H-bonds or the strength of the H-bonds compared to X-bonds? HBs and halogen bonds (XBs) are not of completely equivalent strength, we do not believe that you can directly conclude that HBs are dominant. They are the most common binding type, but without evaluating the relative strength, you cannot determine which are dominant.

Response: We thank the reviewer for this important and constructive comment. We agree that our original wording was potentially misleading. The reported value of 74% was obtained from a statistical count of all identified non-covalent interactions (including hydrogen bonds and halogen bonds) across the sampled cluster configurations, rather than from a comparison weighted by interaction strength. We agree that without evaluating the relative binding energies, it is not rigorous to conclude that hydrogen bonds are energetically "dominant." They are, however, the most prevalent interaction type by count in this system. We have revised the text accordingly:

On lines 135-136 (now on lines 142-143), we have replaced "*HBs are dominant, accounting for up to 74%*" with "*HBs are the most prevalent interaction type, constituting ~74% of all identified non-covalent interactions*".

Lines 135-147: You comment/conclude on the structures of your clusters. We are missing some discussion on how these structures relate to structures in literature. Did your analysis here bring additional information to light not seen in your previous studies? Or is it confirming bonding patterns previously seen in other studies? Here we are thinking of studies that use the same methods as you and those who use different methods. It could be interesting to contrast and

compare.

Response: We thank the reviewer for this valuable suggestion. In response to the reviewer's comment, we conducted a series of comparisons between the IA–MSA–DMA system and the well-established IA–DMA binary system, as it helps to highlight the unique structural features arising from the inclusion of MSA. We have added the following comparative content in the revised manuscript (lines 145-146, page 5):

"*On the contrary, in the binary IA–DMA system, N–H···O HBs represent a slightly lower proportion (~60%) and are exclusively formed between IA and DMA*."

Additionally, the original sentence "*Given that MSA (pK_a = –1.9) is a stronger acid than IA (pK_a = 0.8), DMA preferentially undergoes protonation by MSA, forming the $CH_3SO_3^-$–$DMAH^+$ ion pair*" has been revised to:

"*Another distinct feature compared to the binary IA–DMA pathway is the preferential protonation of DMA by the stronger acid MSA (pKa = –1.9 vs. 0.8 for IA), leading to a dominant $CH_3SO_3^-$–$DMAH^+$ ion pair in the ternary system. This provides a different anionic center ($CH_3SO_3^-$) for interaction compared to the IO_3^-–$DMAH^+$ pair within the binary IA–DMA system*."

Line 146-147: *"These results indicate that IA, MSA, and DMA are capable of forming stable molecular clusters via HBs and XBs, accompanied by acid-base reactions that produce ion pairs."*

I would be a bit careful with this statement, as the structures and existence of HBs and XBs does not explicitly tell you anything about the "stability" of the clusters.

Response: Thanks for this careful observation. As the reviewer correctly notes, we agree that describing the clusters as "stable" based solely on structural analysis is premature, as stability is a thermodynamic property best quantified by binding free energies. To address this, we have revised the statement on line 146-147 (now on lines 157-159) to accurately reflect our findings, as shown below:

"*These results indicate that IA, MSA, and DMA can form molecular clusters stabilized by a network of HBs and XBs, accompanied by acid-base reactions that produce ion pairs.*"

---

4) The Cluster Stability Section

Lines 156-158: You have the critical cluster $(IA)_2(DMA)_1$ growing into $(IA)_3(DMA)_1$ and $(IA)_2(MSA)_1(DMA)_1$. These clusters are a somewhat "acid-heavy". We suggest that you comment on this aspect either here and/or later during the cluster formation pathway section, because as shown in fig. 5a, your outgrowing clusters are also acid-heavy with a 2:1 ratio. Hence, this finding could be an artifact of the chosen systems to study. It has previously been a topic of discussion whether the clusters should be growing along a 1:1 ratio between acid and base or otherwise.

Response: The reviewer's suggestion is professional and critical. As the reviewer correctly pointed out, the critical and growing clusters identified in our system exhibit "acid-heavy" stoichiometries (e.g., $(IA)_2(DMA)_1$, $(IA)_3(DMA)_1$, and $(IA)_2(MSA)_1(DMA)_1$), a pattern that is also reflected in the outgrowing clusters shown in Fig. 5a.

The cluster growth pathway with an acid-base ratio of 2:1 is consistent with previous findings for the nucleation of iodic acid (IA) (Xia et al., 2020; Ning et al., 2022). As highlighted in prior studies (Xia et al., 2020), because IA is a weaker acid ($pK_a \approx 0.8$) compared to strong acids like H_2SO_4 or HNO_3, a single IA molecule is insufficient to fully stabilize a base like ammonia (NH_3) or dimethylamine (DMA) through proton transfer. Clusters with a 1:1 acid-base ratio are relatively unstable and tend to evaporate the base molecule. In contrast, clusters with a 2:1 or higher ratio, where two acid molecules cooperatively stabilize one base molecule, exhibit significantly greater thermodynamic stability. This "acid-heavy" situation also applies to the IA–NH_3 and IA–DMA systems.

Accordingly, for the IA–MSA–DMA system studied here (Fig. 5a), scenarios with acid-base ratios ≥ 1:1 were explicitly considered to include a wider range of potential nucleation clusters and formation pathways. As a result, nucleation driven by the moderately acidic IA

differs from the 1:1 acid–base cluster growth driven by strong acids such as sulfuric acid, instead following pathways of base stabilization by multiple acids, i.e., cooperative multi-acid synergistic nucleation.

---

5) The Cluster Formation Rate

Lines 58-59: You define your cluster system such that only 1:1 acid: base ratio and above is considered. Thus, you bias your simulation towards more acid-heavy systems by not allowing base-heavy systems. This should be commented upon.

Response: We thank the reviewer for the insightful observation. The reviewer is correct that in defining our cluster system, we only considered cases where the acid: base ratio is greater than or equal to 1:1 (i.e., excluding "base-heavy" systems). This choice was based on well-established evidence from previous studies of atmospheric nucleation systems, which consistently show that clusters with excess base ("base-heavy" systems) are thermodynamically unstable and tend to rapidly evaporate the base molecule under atmospheric conditions (Myllys et al., 2019). Furthermore, our previous study also indicated that for iodine-containing acid-base systems, the Gibbs formation energy of the clusters with more acid and less base is significantly lower than that of the cluster with more base and less acid (Ning et al., 2022). The base-heavy clusters are unstable and unlikely to persist to participate in or contribute to nucleation under atmospheric conditions; consequently, we did not consider them, as our aim is to reveal the main pathways that influence nucleation. Following the reviewer's suggestion, we have added the following clarification in the revised manuscript (lines 69-72, page 3):

"*We considered only clusters in which the number of acid molecules equal to or greater than that of base molecules, as prior experimental and observational studies indicate that clusters with excess base are generally thermodynamically less stable and inefficient for nucleation under atmospherically relevant conditions (Myllys et al., 2019; Ning et al., 2022).*"

Limited cluster size: It would also be prudent to consider the effect of the limited system size

on the nucleation rate obtained from ACDC. Limiting the system size will lead to an overestimation of the calculated nucleation rate compared to the "real" nucleation rate. See for example Kubečka et al. 2023 (https://doi.org/10.1021/acs.jpca.3c00068) or Besel et al. 2020 (https://dx.doi.org/10.1021/acs.jpca.0c03984)

Response: We thank the reviewer for raising the point regarding the potential impact of limited system size on the calculated nucleation rates in ACDC simulations. We acknowledge that the limited system size tends to overestimate the calculated nucleation rate (J) compared to larger systems that better approximate the size of observed nucleated particles, as discussed in the provided reference (Kubečka et al., 2023; Besel et al., 2020).

As noted by Kulmala et al. (2013), the critical cluster size for atmospheric nucleation typically falls within the range of 1.1–1.9 nm. In the present work, the largest clusters included in the ACDC simulations consist of up to six molecules, corresponding to an effective size of ~1.2 nm. This size is consistent with reported critical cluster for atmospheric nucleation, which typically fall in the size range (1.1–1.9 nm). Further cluster dynamic analysis further confirms that, at this system size, the collision rates exceed the evaporation rates, indicating that the largest clusters are sufficiently stable to further cluster growth, indicating that the current system size is large enough (see more details in https://github.com/tolenius/ACDC/blob/main/ACDC_Manual_2022_11_18.pdf).

Regarding the impact of expanding the system size on the calculated nucleation rate, Kubečka et al. (2023) reported only "a small drop in particle formation rate" when extending the simulation scheme from 3 × 3 to 4 × 4. This suggests that while a limited system size may lead to a slight overestimation of the absolute nucleation rate, the effect is relatively minor and does not alter the overall trends or mechanistic conclusions. Accordingly, we have added a brief discussion of this limitation in the revised manuscript (lines 96-102, page 4):

"*Furthermore, in our ACDC simulations, the largest clusters considered consist of six molecules (~1.2 nm), which falls within the reported atmospheric nucleation critical cluster sizes of 1.1–1.9 nm (Kulmala et al., 2013). The current system size is large enough because the largest cluster included is stable, with its collisions dominating evaporation. While a limited*

system size can, in principle, lead to a modest overestimation of the nucleation rate, computational studies indicate that expanding the scheme (e.g., from 3 × 3 to 4 × 4) yields only a minor change in the particle formation rate (Kubečka et al., 2023). This suggests that the cluster size employed here is sufficient for capturing the relevant nucleation behaviour; therefore, the present results are consequently reasonable."

Line 185: You compare MSA-DMA with IA-DMA at the same concentration level of acid. This made me curious, is the correlation (if any) between MSA and IA known? Would we expect them to be at the same level in the same regions, because as shown by Chen et al. that you cite for your MSA, it is much more ubiquitous in the southern hemisphere.

Response: We thank the reviewer for this thoughtful question. The reviewer is correct that actual atmospheric concentrations of MSA and IA are governed by distinct sources and environmental factors and may not co-occur at equal levels in the same region.

Our comparison of the MSA–DMA and IA–DMA systems at equal acid concentrations is intended to assess the intrinsic nucleation efficiency of the two binary acid–base systems, independent of their ambient concentrations. As the reviewer correctly notes, a comparison of their actual nucleation effects should indeed consider the precursor concentrations under real atmospheric conditions. In the revised manuscript, we have added a brief clarification to acknowledge this point (lines 205-208, page 8):

"*It should be noted that this comparison is made under equal acid concentrations to evaluate their nucleation efficiency and does not assume equal atmospheric abundances of IA and MSA. Their atmospheric concentrations are influenced by distinct sources and environmental factors, resulting in temporal and spatial heterogeneity.*"

SA vs. MSA: As far as we remember SA is in general a stronger nucleator than MSA. How does your results here compare to the IA-SA-DMA system as previously studied by for example Ning et al. 2024 (https://doi.org/10.1073/pnas.2404595121). In addition, it would be relevant

to note the temperature dependence on the formation of SA/MSA from DMS oxidation here as well.

Response: We thank the reviewer for this relevant and constructive suggestion regarding the comparison with the IA–SA–DMA system and the role of temperature. Following the reviewer's advice, we have performed a comparative analysis of the IA–MSA–DMA and IA–SA–DMA ternary nucleation systems.

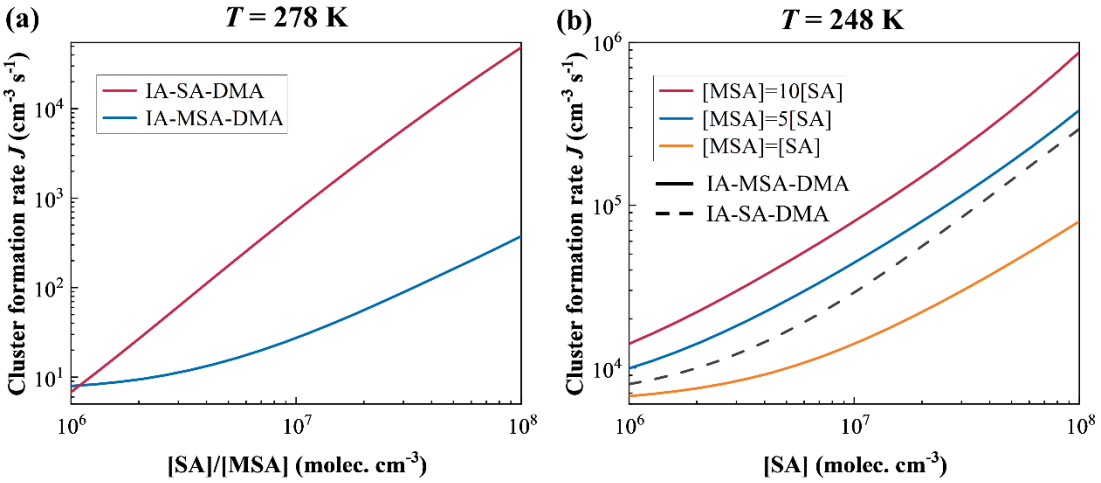

Figure R1. Cluster formation rates J (cm^{-3} s^{-1}) of the IA–SA–DMA and IA–MSA–DMA systems as a function of [SA] or [MSA] at **(a)** 278 and **(b)** 248 K. Key fixed conditions: [IA] = 10^7 molec. cm^{-3}, [DMA] = 0.25 pptv, CS = 2.0×10^{-3} s^{-1}.

As shown in Fig. R1, we compared the nucleation rates of the IA–SA–DMA and IA–MSA–DMA systems at 278 K and 248 K. At 278 K, the IA–SA–DMA pathway exhibits significantly higher nucleation rates, exceeding those of IA–MSA–DMA by up to two orders of magnitude, consistent with SA being a stronger nucleator. As the reviewer rightly notes, the atmospheric oxidation of DMS to form MSA is highly temperature-dependent, with lower temperatures favoring MSA formation (Chen et al., 2023). To reflect this realistic scenario, we compared the systems under more representative cold conditions, specifically at T = 248 K. Under this temperature, when [SA] = [MSA], the nucleation rate of the IA–MSA–DMA system remains significantly lower than that of the IA–SA–DMA system. However, when the MSA concentration is increased to [MSA] = 5[SA] and [MSA] = 10[SA], the nucleation rate of the

IA–MSA–DMA pathway becomes higher.

These results confirm that while the SA-driven pathway is effective, the IA–MSA–DMA mechanism we identified is highly competitive, especially in cold environments where MSA production is enhanced. This underscores that MSA can be a co-dominant driver of iodine-mediated nucleation in specific marine regions.

Lines 200-204: *"This mechanism serves as a critical yet overlooked source of fresh particles in the MBL."*

We believe the conclusion here are a bit overexaggerated and not entirely backed up by your results. Please tone down the relevance in light of the results.

Response: Thanks for the reviewer's valuable comment. We agree that describing the IA–MSA–DMA mechanism as "a critical yet overlooked source" may overstate its atmospheric significance based solely on our modelling results. We have therefore revised the manuscript to more accurately reflect the scope of our findings. The sentence now reads:

"*This mechanism represents a potentially important and previously overlooked NPF nucleation pathway in the MBL.*"

---

6) Synergistic Nucleation of IA, MSA, and DMA

Enhancement factor: You define the enhancement factor as: R = J(IA-MSA-DMA)/J(IA-DMA). However, you are referring to the synergistic effect of co-nucleation. Thus, would it not be more appropriate to define it as: R = J(IA-MSA-DMA) /(J(IA-DMA) + J(MSA-DMA)) = J(IA=x, MSA=y, DMA=z) / (J(IA=x, MSA=0, DMA=z) + J(IA=0, MSA=y, DMA=z)). In this way you isolate the synergy effect from the effect of just adding more nucleation precursors. Technically the IA-MSA, and the self-nucleation of IA, MSA, DMA should also be there, but it is relatively easy to dismiss these as irrelevant at atmospherically relevant concentrations.

Response: Thanks for the reviewer's thoughtful and constructive comments. As the reviewer

pointed out, a more rigorous definition would be R = J(IA–MSA–DMA) / [J(IA–DMA) + J(MSA–DMA)], ideally with matched the synergistic effect of co-nucleation.

Following the reviewer's suggestion, we have redefined the enhancement factor in the revised manuscript. Furthermore, we performed additional calculations to assess the practical impact of this refined definition. We calculated the nucleation rates for the IA–MSA–DMA, IA–DMA, and MSA–DMA systems. The results, presented in the Figure R2, reveal a key finding: J(MSA–DMA) is consistently 4 – 7 orders of magnitude lower than J(IA–DMA) under our studied conditions. Consequently, the contribution of J(MSA–DMA) to the denominator [J(IA–DMA) + J(MSA–DMA)] can be negligible. As shown in the figure, the curves for the originally used R_1 = J(IA–MSA–DMA) / J(IA–DMA) and the refined R_2 = J(IA–MSA–DMA) / [J(IA–DMA) + J(MSA–DMA)] are completely overlap.

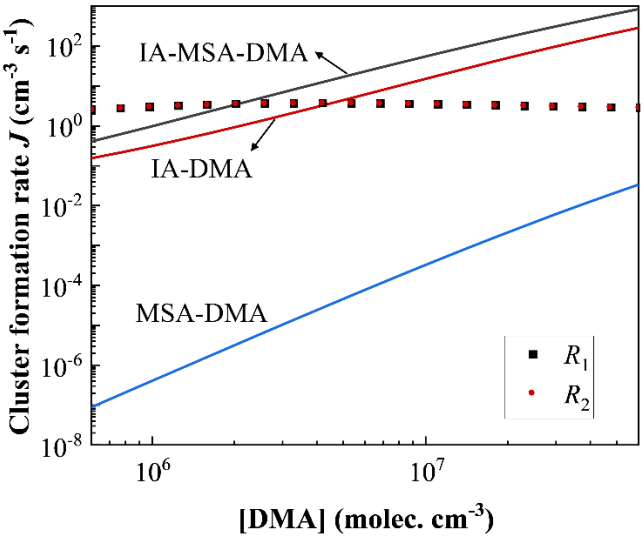

Figure R2. Variation in cluster formation rates for the IA–MSA–DMA, IA–DMA, and MSA–DMA nucleation, along with the corresponding enhancement factors R_1 = J(IA–MSA–DMA) / J(IA–DMA) and R_2 = J(IA–MSA–DMA) / [J(IA–DMA) + J(MSA–DMA)], as a function of [DMA] = 6 × 10^6 – 6 × 10^7 molec. cm^{-3}.

Overall, redefining R_2 does not alter the results or conclusions of this study. Nevertheless, we have adopted this refined definition in the revised manuscript, as it provides a more appropriate and robust metric, particularly for systems in which the two terms in the

denominator are of comparable magnitude, i.e., systems involving competing pathways. We therefore thank the reviewer for this constructive suggestion, which is important not only for the present work but also for future studies.

Lines 224-225: *"IA-MSA-DMA synergistic nucleation is most effective in iodine-limited, sulfur-, and nitrogen-rich regions."*

Perhaps rephrase *"most effective"* to *"most relevant"*. IA-MSA-DMA is also enhanced by [IA], it is just less impacted by limited [IA] compared to IA-DMA.

Response: We thank the reviewer for the careful wording suggestion. We agree that "most relevant" more accurately conveys our intended meaning than "most effective." We have revised the sentence accordingly:

"*IA–MSA–DMA synergistic nucleation is most relevant in iodine-limited, sulfur-, and nitrogen-rich regions.*"

---

7) Cluster Formation Pathway Section

Line 234: *"This part of pathways are similar to that revealed by Ning et al. (2022b)."*

Isn't the data also taken from Ning et al. (2022b)? In that case I would explicitly write that this is the finding from Ning et al.

Response: Thanks for this careful observation. We confirm that all data presented in this section are derived from our independent simulations of the ternary IA–MSA–DMA system. The statement was intended to highlight that the IA–DMA binary pathway emerging from our ternary clustering simulations is similar to the mechanism previously reported by Ning et al. (2022b) for the binary IA–DMA system. We have revised the sentence to state this explicitly. The corrected text now reads:

"*The dominant nucleation mechanism identified in the ternary IA–MSA–DMA system involves two types of pathways: the ternary IA–MSA–DMA pathway and the binary IA–DMA*

pathway, the latter of which is similar to the pattern reported by Ning et al. (2022b)."

Line 256: You refer to fig. S5, we believe you mean S4. We suggest you go through the references to the SI and double check the figure numbers.

Response: We thank the reviewer for the careful reading and for pointing out this error. The reviewer is correct—the reference should indeed be to Fig. S4. We apologize for this oversight and have corrected the citation in the revised manuscript. Additionally, we have carefully reviewed all references to figures in the Supporting Information to ensure accuracy.

Further on line 256: You refer to a distinct change in growth pattern. There is no discussion of this change in either the main manuscript nor SI. Please comment on what you meant by this in either the manuscript or SI.

Response: Thanks for careful reading. As the reviewer pointed out, the "distinct change in growth pattern" mentioned on line 256 was not elaborated upon. We are referring to the change in the dominant growth pathway with temperature in the IA–MSA–DMA system, as revealed by our ACDC simulations.

Specifically, at T = 278 K, cluster growth of IA–MSA–DMA system proceeds primarily via the formation and outgrowth of the $(IA)_2(MSA)_2(DMA)_2$ cluster. In contrast, at the higher temperatures of 288–298 K, the dominant clustering pathway shifts to growth initiated by the $(IA)_1(MSA)_2(DMA)_3$ cluster. This change reflects differences in the preferred growth pathways under different temperature conditions. We have added a brief explanation of this point in the revised manuscript (lines 289-291, page 12). The added text will read:

"*Specifically, the dominant growing cluster shifts from $(IA)_2(MSA)_2(DMA)_2$ at 278 K to $(IA)_1(MSA)_2(DMA)_3$ at 288–298 K, indicating temperature would influence the cluster growth pathway.*"

Lines 268-269: You comment that the IA concentrations decrease significantly at high latitudes with lower temperatures and cite He et al. 2021. Do they show this? In the main manuscript they primarily discuss nucleation rates, but in fig. S9 and S10 there does not seem to be a clear latitude dependence. For example, the Beijing, Nanjing, and Réunion measurements are significantly lower than Greenland and Ny Ålesund. In addition, Helsinki could be said to exhibit comparative concentrations to Greenland and Ny Ålesund.

Response: We thank the reviewer for this careful and correct observation. The reviewer is right that the data presented in He et al. (2021) does not directly support a clear latitudinal gradient in IA concentrations. We inappropriately cited this reference and have therefore replaced it with the study by Takashima et al. (2022), which provides systematic ship-based measurements of iodine monoxide (IO) from the Arctic to the Southern Hemisphere. Their work consistently shows lower IO levels at higher latitudes (Figure 4). Since IO is a key intermediate in the formation of iodic acid (IA), and CLOUD experimental evidence indicates a strong correlation between IA concentrations and IO radical levels (Finkenzeller et al., 2023), IA concentrations are likely to follow similar latitudinal trends as IO. The sentence in the manuscript has been revised accordingly and now reads:

"*…while IA concentrations tend to decrease at higher latitudes with lower temperatures, as reflected in the observed decline of iodine monoxide (a key IA precursor) with increasing latitude (Takashima et al., 2022)*."

---

8) Comparison with Field Observations

8a) The simulated nucleation rates are compared to the measurements at Marambio and Aboa:

For Marambio, looking at fig. 4 and 5 in Quéléver et al., the median hourly concentrations were around 3*10^5 (according to fig. 5) with many measurements of around 10^6, with drops below 10^5 only during the night (according to fig. 4) Looking at your fig. 6a, IA-DMA would already be within the field observation range at an [IA] of 3*10^5.

Response: We thank the reviewer for the careful examination of the comparison between our simulated nucleation rates and the field observations at Marambio (Quéléver et al., 2022). We agree that Figure 5 of Quéléver et al. (2022) shows hourly median IA concentrations around 3×10^5 molec. cm^{-3}, with frequent values near 10^6 molec. cm^{-3} during daytime and lower values at night. Under such conditions, the IA–DMA binary pathway indeed reaches the lower bound of the observationally inferred range, as evident in our Fig. 6a.

To better represent the full variability of the measurements, including both daytime and nighttime conditions, we have expanded the IA range in Fig. 6a to 10^4 – 10^6 molec. cm^{-3} (as seen in the Figure 4 of Quéléver et al. (2022)). Within this broader range, in fact, IA–DMA nucleation only overlaps with the field observations at the high-IA levels, whereas IA–MSA–DMA ternary pathway remains consistent with the observed nucleation rates across nearly the entire IA concentration range.

In fact, ternary IA–MSA–DMA nucleation inherently includes IA–DMA pathway, and the two are not separate. These results indicate that under high-IA concentrations, the contribution of the IA–DMA pathway becomes increasingly prominent and can account for a portion of the nucleation rate. Conversely, at lower IA levels, the effect of MSA is pronounced, and ternary nucleation driven by synergistic effects can effectively capture the observed nucleation rates. Overall, MSA-enhanced ternary nucleation appears capable of reproducing nucleation rates across the observed range of IA concentrations, particularly in the high-rate regime, which is not fully captured by the IA–DMA binary mechanism, even at the highest IA levels.

We have updated the text and figure (Fig. 6(a)) in the revised manuscript (lines 320-326, page 13) as following:

"*Even at the lower bound of [MSA] (10^6 molec. cm^{-3}, lower orange solid line), the simulated formation rates still match or exceed the minimum observed value (0.12 cm^{-3} s^{-1}, lower black dashed line). Moreover, at lower IA levels, the effect of MSA is pronounced, and ternary nucleation driven by synergistic effects can effectively capture the observed nucleation rates. Conversely, under high [IA], the contribution of the IA–DMA pathway becomes increasingly prominent and can account for a portion of the nucleation rate. Overall, the MSA-*

enhanced ternary nucleation appears capable of reproducing the nucleation rates observed at Marambio across the measured range of [IA], particularly under high-rate conditions. Even at the highest IA levels, this reproduction cannot be fully captured by the IA–DMA binary mechanism alone."

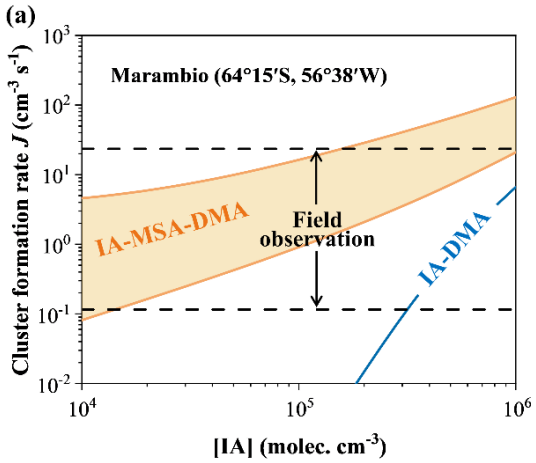

Figure 6. (a) Comparison with the simulated cluster formation rate (J, cm^{-3} s^{-1}) and field observations under the ambient conditions at Marambio (T = 273 K, CS = 10^{-4} s^{-1}, [IA] = 10^4 – 10^6 molec. cm^{-3}, [MSA] = 10^6 – 10^7 molec. cm^{-3}, and [DMA] = 2.0 pptv).

For Aboa: fig. S3 in Xavier et al. shows quite stable [IA] that don't go below 4*10^5. Here it is true that IA-DMA will significantly undershoot the field observations. But at the same time, while your IA-MSA-DMA is starting to overshoot the field observations event at the minimum of 4*10^5.

Response: We thank the reviewer for this insightful comment. It is true that the findings from Xavier et al. suggest a relatively stable [IA] around and above 4 × 10^5 molec. cm^{-3}. Under such conditions, our simulations indicate that the binary IA–DMA pathway substantially underestimates the observed nucleation rates, while the upper bound of the ternary IA–MSA–DMA pathway begins to exceed the measurements, as correctly noted by the reviewer.

Our intention was to evaluate nucleation behaviour over the broader range of IA concentrations reported for the Aboa site. In addition to Xavier et al., measurements by Jokinen

et al. (2018) indicate that IA concentrations at Aboa can vary from ~10^5 to 10^6 molec. cm^{-3}, with frequent occurrences below 10^5 molec. cm^{-3} (shown in their Fig. 1c). Over this wider range of [IA], the IA–MSA–DMA mechanism remains consistent with the observed nucleation rates across a larger fraction of the measurements than the binary IA–DMA pathway alone.

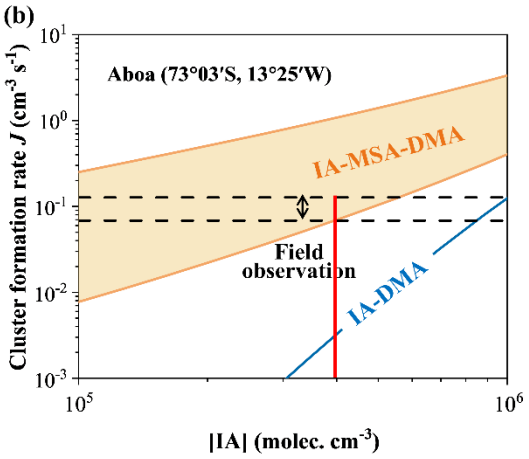

Figure 6. (b) Comparison with the simulated cluster formation rate (J, cm^{-3} s^{-1}) and field observations under the ambient conditions at Aboa (T = 268 K, CS = 10^{-4} s^{-1}, [IA] = 10^5 – 10^6 molec. cm^{-3}, [MSA] = 10^6 – 10^7 molec. cm^{-3}, and [DMA] = 0.055 pptv).

According to our study, the ternary IA–MSA–DMA mechanism is most directly applicable for explaining the observed nucleation rates under conditions of lower to moderate IA concentrations (closer to ~10^5 molec. cm^{-3}), where the binary pathway is overall insufficient. Indeed, as the reviewer points out, the upper bound of the simulated IA–MSA–DMA nucleation rate exceeds the observed rates at [IA] = 4 × 10^5 molec. cm^{-3} (red line in Fig. 6(b)). However, the lower simulated values remain within the measurements (dashed lines), indicating that the ternary mechanism provides a better description of the nucleation rates than the IA–DMA binary pathway.

Furthermore, for Marambio and Aboa.

You plot that the nucleation rates observed in the field at Marambio are between 10^-1 and just over 10^1. Where in the Quéléver study are you getting these numbers? At which size are these

formation rates obtained (J_1.5, J_2, J_3, J_5, or J_10?) Looking at table 1 and figure 6c, we would expect significantly different formation / nucleation rates.

Likewise, for Aboa (Xavier et al 2024), from where do you get the nucleation rates that are around 10^-1? As far as we read the article, it does not present any experimental formation rates, or any simulated formation rates that correspond to that number. Furthermore, Xavier et al is not the original source for the 2015 Aboa campaign, that is Jokinen et al. 2018 (https://doi.org/10.1126/sciadv.aat9744). In Jokinen et al, we did find measured formation rates from the period of 07/01/2015 to 09/01/2015 that is reported in Xavier et al. In Jokinen et al. 2018 table S2, they report values at J_1.5 to be 0.09 to 0.11 (0.07-0.13 for the entire period) or J_1.5, extrap as 0.05-0.12. As far as we read fig. 6, you have set the bounds for the field observations at 0.07 to just over 0.1. Thus, you must have used the values reported in Jokinen et al. 2018, but without citing them?

In general: it should be much clearer which observations you use (time-period, which formation rate it is, what is the source).

Response: We thank the reviewer for their careful and detailed examination of the observational data sources. We fully agree that it should be stated more explicitly which observational datasets are used, including the time period, formation-rate definition, and original source. This comment is particularly valuable, as it helps improve the transparency and reliability of our results.

For Marambio: The nucleation rate range shown in Fig. 6a of our manuscript for the Marambio field data (approximately 10^{-1} to just over 10^{1} cm^{-3} s^{-1}) is taken directly from Figure 6c in Quéléver et al. (2022), corresponding to particles with diameters >1.5 nm ($J_{1.5}$). As correctly noted by the reviewer, formation rates can differ depending on the chosen size threshold (e.g., J_2, J_3, J_5). Here, we selected $J_{1.5}$ as the most appropriate metric for comparison because the nucleating clusters resolved in our ACDC simulations correspond most closely to this size range, making $J_{1.5}$ the most directly comparable quantity to our theoretical results.

For Aboa: As the reviewer correctly pointed out, the article by Xavier et al. (2024), which we previously cited, does not contain the primary observed nucleation rate data for the 2015 Aboa

campaign. The field-observation range in Fig. 6b is based on the $J_{1.5}$ values reported by Jokinen et al. (2018), specifically those listed in Table S2 (approximately 0.07 – 0.13 cm^{-3} s^{-1} for the relevant period). We acknowledge that the omission of this original reference in the initial version was an oversight. This has now been corrected by explicitly citing Jokinen et al. (2018) as the source of the Aboa observational constraints.

To address the reviewer's general concern, we have revised the caption of Fig. 6 to specify the formation-rate definition and data sources as follows:

"*The dashed field-observation ranges for J at Marambio (0.1 – 24 cm^{-3} s^{-1}) and Aboa (0.07 – 0.13 cm^{-3} s^{-1}) are based on the reported $J_{1.5}$ values from Quéléver et al. (2022) and Jokinen et al. (2018), respectively.*"

Furthermore, you use [MSA]=10^6-10^7 i.e. MSA between roughly 0.1 to 1 ppt. However, many of the studies you cite (Chen et al. 2018, Chen et al. 2023), would put the MSA concentrations much higher in the southern hemisphere (10-40 ppt).

Response: Thanks for raising this important point. The reviewer correctly notes that modelling studies, such as those by Chen et al. (2018, 2023), can indicate MSA concentrations reaching 10–40 ppt in certain Southern Hemisphere scenarios.

The MSA concentration range adopted in our comparative simulations in Fig. 6 (10^6 – 10^7 molec. cm^{-3}, corresponding to approximately 0.1–1 ppt), is based on observational constraints for the Marambio and Aboa sites, rather than on modeled values. To our knowledge, available field measurements at these Antarctic coastal locations indicate that MSA concentrations are typically within this order of magnitude.

Accordingly, our simulations aim to perform a site-relevant comparison between the simulated nucleation rates constrained by observations and field measurements under ambient precursor levels.

Also, for the rest of the paper: why only up to 10^8 (roughly 10 ppt) MSA, if you are aiming to compare to measurements in the southern hemisphere?

Response: Thanks for raising this important question. Our choice to simulate MSA concentrations up to ~10^8 molec. cm^{-3} is deliberate and based on the representative atmospheric conditions. Field observations by Yan et al. (2019) reported an average gaseous MSA concentration of 3.3 ± 1.6 pptv (up to the order of 10^8 molec. cm^{-3}) over the Southern Ocean, which is a recognized hotspot for marine biological activity and DMS emissions. This demonstrates that our chosen concentration range can effectively encompass the typical concentrations commonly observed even in such high-DMS-emission regions.

Although modelling studies suggest that MSA concentrations may reach 10–40 pptv in specific regions (Chen et al., 2018), the observational studies indicate that long-term, boundary-layer measurements of gas-phase MSA are typically found at levels comparable to or lower than those of sulfuric acid (H_2SO_4), on the order of 0.1 to a few pptv (Eisele and Tanner, 1993; Berresheim et al., 2002). Therefore, an upper limit of 10^8 molec. cm^{-3} may cover a broad and representative concentration range sufficient to assess the potential importance of this mechanism in marine boundary layer.

Generally: Your simulations already overestimate the field observations even before considering the many other possible nucleation pathways, hydration of clusters, and ions. Would this not be an indication that your method may have too stable clusters? I.e. you are not "leaving room" for all the other things that could contribute to and assist nucleation.

Response: Thank you for this insightful comment. Our high-concentration scenarios presents that the simulated nucleation rates can approach or exceed field measurements. Herein, we emphasize that this behaviour does not imply that our calculations produce unrealistically "too stable" clusters.

The overestimation of nucleation rates arises primarily from the intentional use of idealized, concurrent upper-range concentrations of IA, MSA, and DMA. However, in the real

atmosphere, these precursors exhibit strong temporal variability; thus, they are unlikely to simultaneously reach their upper levels. Due to the lack of high-time-resolution measurements of all relevant precursors at the same field sites, our simulations are designed to explore the upper-limit nucleation potential of the IA–MSA–DMA mechanism rather than to reproduce instantaneous atmospheric conditions.

As a result, a gap between simulated nucleation rates and field observations may persist, which likely reflects the influence of additional processes not explicitly included in our simulations, such as other possible nucleation pathways, cluster hydration, and ion-induced effects. Importantly, the inclusion of these pathways may not lead to an enhancement of nucleation. These processes likely compete for shared nucleating precursors, thereby consuming available clustering agents and potentially suppressing, rather than enhancing, the effective nucleation rate of a given pathway. We note that exploring the contributions and potential competition among all relevant pathways, including cluster hydration and ion effects, remains an important direction for future studies, which will help to further clarify the overall picture of atmospheric nucleation.

We have added a corresponding note in the revised manuscript (lines 333-339, page 12) as following:

"*It should be noted that the nucleation rates presented here, particularly at the upper end of the studied concentration ranges, represent the theoretical results under ideal conditions of concurrently high precursor levels. In the marine atmosphere, temporal and spatial variations in the concentrations of IA, MSA, and DMA will modulate the rates. Nevertheless, our proposed synergistic mechanism of the ternary IA–MSA–DMA nucleation provides a critical mechanistic understanding for periods and regions where these precursors co-exist at significant levels.*"

---

9) Minor Comments:

Line 26-27: You write: *"Notably, aerosol are the primary source of uncertainty in climate forcing. And aerosols originate …"*. We suggest removing the *"And"*.

Response: Based on the reviewer's suggestion, the word "*And*" has been removed in the revised

manuscript.

Line 114: For the MSA concentration you cite *"Ning et al., 2022a"*, however this is a quantum chemistry nucleation study?

Response: Thank you for pointing this out. The reviewer is correct that Ning et al. (2022a) is a quantum chemical nucleation study rather than an observational or measurement-based reference. We originally cited this work because our simulations adopted a similar MSA concentration range, and the citation was intended solely to provide contextual consistency with previous theoretical studies. However, we agree that citing a quantum chemical study in support of atmospheric MSA concentrations may be misleading. To avoid any potential confusion, we have removed the citation to Ning et al. (2022a) in the revised manuscript and now rely exclusively on observational studies where concentration values are discussed.

Line 153: remove *"formed"* from the sentence

Response: Based on the reviewer's suggestion, the word "*formed*" has been removed in the revised manuscript.

Line 166 and 171: You write that lower [IA] favors the IA-MSA-DMA pathway. We feel that it would be more correct to say that the pathway is comparatively more favorable at lower [IA], because lower [IA] would result in the IA-DMA clusters becoming unfavorable faster than IA-MSA-DMA. Thus, none of them are *"favored"*, some are just less disfavored.

Response: We thank the reviewer for this precise wording suggestion. We have revised the text accordingly.

In the revised manuscript, the statement on line 166 (now on lines 183-184) now reads: "*This suggests that, unlike [MSA], lower [IA] makes the IA–MSA–DMA pathway comparatively less disfavored than the IA–DMA pathway*."

In the revised manuscript, the statement on line 171 (now on lines 188-189) now reads: "*These results indicate that under the conditions where MSA and DMA are abundant but IA is limited, the IA–DMA pathway becomes thermodynamically unfavorable more rapidly, making the IA–MSA–DMA pathway relatively more favorable.*"

Line 204: You should probably add that it is a yet overlooked *potential* source of fresh particles. This is still only at a computational, while you compare to measurements, there is no comparison to experiments isolating the effect of the limited IA-MSA-DMA system.

Response: We thank the reviewer for this suggestion. We have revised the sentence on line 204 (now on lines 222-223) accordingly. The text now reads:

"*This mechanism represents a potentially important and previously overlooked NPF nucleation pathway in the MBL.*"

Line 207: access -> assess

Response: We thank the reviewer for the careful observation. The word "*access*" has been corrected to "*assess*".

Fig. 6: We assume that the shaded region is defined by simulations at 10^6 MSA and 10^7 MSA? This should be written in the text / figure caption.

Response: You are absolutely right. The shaded region in Fig. 6 is defined by simulations at [MSA] range of 10^6 – 10^7 molec. cm^{-3}. Based on the reviewer's suggestion, the caption for Fig. 6 in the revised manuscript has been updated with the following clarification: "*The shaded area corresponds to the nucleation rates simulated at [MSA] = 10^6 – 10^7 molec. cm^{-3}.*"

Referee #3:

Li et al. have applied quantum chemical calculations and cluster dynamics simulations to investigate the IA–MSA–DMA ternary nucleation system at molecular levels and assess the importance of IA–MSA–DMA nucleation mechanism in polar marine regions (Marambio and Aboa). The outcome of this study will be providing insights from the theoretical aspect of IA–MSA–DMA ternary nucleation mechanism in polar marine environment. Overall, the manuscript is well-written and the results are clearer presented. I have some minor comments as below:

Response: Thanks sincerely for the reviewer's professional and positive comments. We have revised the manuscript accordingly. The detailed point-to-point responses are listed as follows.

---

1) I don't quite understand why the authors need to use "typical sulfur-, iodine-, and nitrogen-bearing chemicals" both in the title and also in the text (i.e., abstract Line 11) instead of more directly stating IA–MSA–DMA system? Is there any specific reason? Sulfur and nitrogen chemicals can be broad, for example, sulfuric acids (H_2SO_4) and nitric acids (HNO_3) can have influence on the nucleation process too.

Response: Thanks for raising this valid point. Our intention in using the phrase "typical sulfur-, iodine-, and nitrogen-bearing chemicals" in the title and abstract was intended to convey that the precursors we investigated represent broad classes of key atmospheric precursors, thereby highlighting the scope of relevant chemical families. We selected MSA and DMA as the specific representatives because they are indeed the dominant and efficient sulfur- and nitrogen-containing nucleating precursors in marine regions. For instance, MSA is generally considered to be produced almost exclusively from the oxidation of marine-derived dimethyl sulfide (DMS) and is often used as a tracer for marine biogenic sources (Zhou et al., 2021). This makes them the most relevant precursors for studying multicomponent nucleation in marine environments.

We acknowledge the reviewer's correct observation that other sulfur/nitrogen compounds like H_2SO_4 and HNO_3 are also important in atmospheric nucleation, yet previous research has

primarily focused on their central role in continental or urban environments. Thus, H_2SO_4 and HNO_3 were not included in our modelling framework.

---

2) Line 21: In the abstract, what do you mean by "helping to explain the missing sources of iodic acid particles"?

Response: Thanks for the reviewer's careful question, which allows us to clarify an important point. Our intended meaning is that the identified IA–MSA–DMA synergistic mechanism represents a previously unknown pathway that contributes to the formation of new particles in marine environments.

To avoid ambiguity and better reflect the broader implications of our work, we have revised the sentence in the abstract. The updated text now reads:

"*...helping to explain the missing sources of marine particles*"

---

3) Line 51-52: Please provide the citations for the "field observations indicate that MSA frequently coexists with IA and DMA in the marine atmosphere". Which studies?

Response: We thank the reviewer for the careful reading. The statement regarding the co-occurrence of MSA, IA, and DMA in the marine atmosphere is supported by the concurrent measurements presented in Salignat et al. (2024). Specifically, their field measurements at the Maïdo Observatory (southern Indian Ocean) demonstrate that these three key precursors—iodic acid (IA), methanesulfonic acid (MSA), and dimethylamine (DMA)—were consistently detected during the 7-day campaign (11–17 April 2018). This simultaneous presence is clearly illustrated in their Figures 8(a) and 8(b), which present the concentration-time profiles of these species. We will add this citation to the revised manuscript at lines 51-52.

---

4) Line 63-64: Maybe I have missed out something, what are different latitudinal marine conditions that have been evaluated in this study? Please be specific.

Response: We thank the reviewer for requesting this clarification. In this study, the "different latitudinal conditions" correspond to the varying meteorological and chemical parameters simulated, specifically the temperatures (representing polar vs. warmer oceans) and precursor concentrations (representing biologically active). In response, we have revised the sentence to more clearly reflect that our mechanistic analysis is based on distinct marine environments. The updated text now reads:

"*Furthermore, by analyzing the nucleation pathway under different marine conditions, we quantify the contribution of IA–MSA–DMA ternary nucleation to particle formation*."

---

5) In the methodology, I did not see any introduction or discussion about the uncertainty of this study. The uncertainties arise from the quantum chemical calculations and from the cluster dynamic simulations should be also included here.

Response: We thank the reviewer for this constructive comment. Following the reviewer's suggestion, we have now included a dedicated discussion on the uncertainties arising from both the quantum chemical calculations and the cluster dynamics simulations in the revised manuscript. According to the benchmark study by Liakos et al. (2020), the mean absolute deviations (MAD) introduced by the DLPNO-CCSD(T) method are typically $\leqq 0.4$ kcal mol^{-1}, with most datasets showing MADs below 0.2 kcal mol^{-1}. Therefore, to account for the uncertainty introduced by the quantum chemical calculations, the calculated Gibbs free energies of cluster formation were adjusted by ±0.2 kcal mol^{-1}. As shown in Fig. S5(a), under the conditions of T = 278 K, CS = 2.0 × 10^{-3} s^{-1}, [IA] = 10^5 – 10^8 molec. cm^{-3}, [MSA] = 10^7 molec. cm^{-3}, and [DMA] = 0.25 pptv, increasing or decreasing the ΔG_{278K} of the cluster by 0.2 kcal mol^{-1} results in only minor changes in the J values, all within one order of magnitude. This indicates that the uncertainty in the quantum chemical calculations has no significant impact on the conclusions of this study. Furthermore, we evaluated the uncertainty arising from the collision rate estimation by varying the collision enhancement factor (sticking factor, SF) on the cluster formation rate J for the IA–MSA–DMA system. As shown in (Fig. S5(b)), varying this factor within a physically reasonable range (from 2.1 to 2.5) leads to minor variation in J,

preserving the overall trends. These sensitivity analyses indicate that the uncertainties introduced by quantum chemical calculations and cluster dynamics simulations do not significantly affect the main conclusions of the current study.

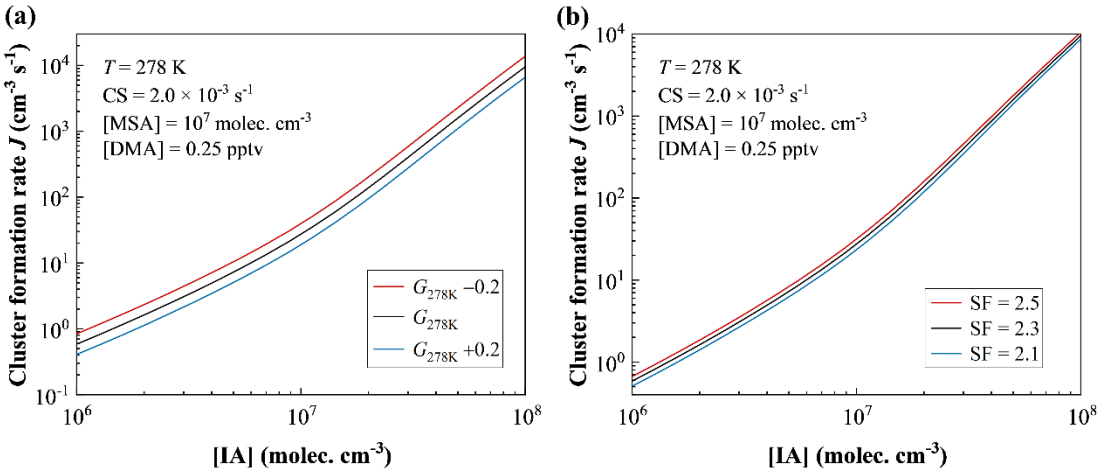

Figure S5. (a) Cluster formation rate J as a function of IA concentration ([IA] = 10^6 – 10^8 molec. cm^{-3}) under different Gibbs free energy values: $\Delta \boldsymbol{G}_{278K}$ (black line), $\Delta \boldsymbol{G}_{278K}$ + 0.2 (blue line), and $\Delta \boldsymbol{G}_{278K}$ – 0.2 (red line). Conditions: $\boldsymbol{T}$ = 278 K, CS = 2.0 × 10^{-3} s^{-1}, [MSA] = 10^7 molec. cm^{-3}, and [DMA] = 0.25 pptv. **(b)** J for the IA–MSA–DMA system under different sticking factor (SF = 2.1 – 2.5) conditions.

Here, we have added the results of J under different Gibbs free energy and sticking factors to the revised supporting information, and for the convenience of the review, we have copied Figure S5 and the corresponding analysis (lines 229-232, page 9 in the revised manuscript) as following:

"*Additionally, to account for potential uncertainties in quantum chemical calculations and cluster dynamic simulations, we also examined the effects of the calculated ΔG of clusters and the enhancement factor (sticking factor, SF) on J. As shown in Fig. S5, under boundary-layer conditions, variations in the ΔG (±0.2 kcal mol^{-1}) (Liakos et al., 2020) of clusters and the SF (2.1 – 2.5) in dynamic simulations lead to only minor changes in J.*"

---

6) Line 110: Please define CLOUD.

Response: We thank the reviewer for the suggestion. CLOUD is the acronym for Cosmics Leaving Outdoor Droplets, and we have added the full term upon its first mention in the revised manuscript (line 124, page 5).

---

7) Figure 3b: It is not explained why only IA–HIO2 system line is shown for the comparison here. Please justify why [IA]/[HIO_2] is fixed at a value of 50 instead of other numbers?

Response: Thanks for raising this helpful point. We will now clarify the rationale behind the selection of the IA–HIO_2 system and the parameter settings, respectively.

(1) Rationale for choosing the IA–HIO_2 system for comparison:

The IA–HIO_2 pathway is a well-established binary nucleation system that has been widely observed and modeled in the marine boundary-layer environments (He et al., 2021; Liu et al., 2023; Zhang et al., 2022). Comparing our ternary IA–MSA–DMA mechanism with this known binary system helps to quantify the relative enhancement brought by the synergistic interaction of multiple marine precursors.

(2) Justification for setting [IA]/[HIO_2] = 50:

This ratio was chosen to represent environmentally relevant conditions. Specifically, field measurements by Sipilä et al. (2016) in marine regions show that during new particle formation events, the peak detected concentration of gaseous IA reached up to 10^8 molec. cm^{-3}, while that of HIO_2 was 2×10^6 molec. cm^{-3}, resulting in a ratio of [IA]/[HIO_2] ≈ 50. Given that IA and HIO_2 originate from the same iodine reservoir, their formation is likely to be highly correlated. Therefore, a [IA]/[HIO_2] ratio of 50 was adopted in our study accordingly.

---

8) Figure 4: Suggest to add information of correlation coefficient (r) for the linear fit to the figure or in the caption.

Response: Following the reviewer's helpful suggestions, we have now added the correlation coefficients (r) for all linear fits in the caption of Figure 4. Specifically, the r values are 0.99 for

the [IA]–rate relationship, 0.98 for the [MSA]–rate relationship, and 0.99 for the [DMA]–rate relationship.

---

9) Line 267-268: Chen et al. (2023) study is mainly based on the calculation and modelling results. Are there measurements that support MSA formation is highly temperature-dependent? If yes, please cite them.

Response: Thanks for the suggestion regarding the observational support for the temperature dependence of MSA. We agree that while Chen et al. (2023) provides a theoretical basis, field evidence is crucial. In addition to this, we cite the observational study by Scholz et al. (2023), which provides direct field evidence. Their measurements at the high-altitude Chacaltaya station show that MSA concentrations are significantly higher in the colder free troposphere than in the boundary layer (see their Fig. 6g), supporting the conclusion that MSA formation is enhanced at lower-temperature conditions. By citing this field evidence alongside the modelling results of Chen et al. (2023), we provide a more robust support for the enhanced MSA formation potential in cold, high-altitude environments.

---

10) Figure 6: Why the concentration of DMA is reported as pptv instead of molecules cm-3? What are the concentrations of MSA being used for the calculation in orange area?

Response: Thanks for raising this question. We will provide the following explanation regarding the units and concentration ranges used in Fig. 6.

(1) DMA concentration in pptv:

We presented DMA concentrations in pptv to align with the convention widely used in field observational studies for amines (e.g., CLOUD experiments and ambient measurements), whereas acid precursors (like IA and MSA) are typically reported in molecules cm^{-3}. This facilitates a direct comparison between our simulation conditions and the concentration ranges reported in the literature for marine environments. Moreover, this mixed usage of acid-base units is also observed in other studies (Almeida et al., 2013; He et al., 2023).

(2) MSA concentration for the shaded area:

The orange-shaded area representing the IA–MSA–DMA nucleation rate is calculated using an MSA concentration range of 10^6 to 10^7 molec. cm^{-3}. These [MSA] values are observationally constrained, derived from field measurements at the Marambio and Aboa stations (Quéléver et al., 2022; Jokinen et al., 2018). We have revised the Fig. 6 caption to explicitly include this concentration range information.

---

11) Line 313: Justify how the study lead to advancing our understanding of NPF events if they are aligning well with field observations?

Response: We thank the reviewer for this critical question regarding the scientific contribution of our study. Indeed, the agreement between our simulations with field observations serves not only to validate the significance of the proposed mechanism but also to help reveal mechanistic insights that are not obtainable through measurements alone.

Specifically, we identify and elucidate the synergistic nucleation of marine-typical precursors (iodine-, sulfur-, and nitrogen-containing species, e.g., iodic acid (IA), methanesulfonic acid (MSA), dimethylamine (DMA)), which enables highly efficient particle formation. Additionally, we reveal the molecular mechanism to constrain chemical transport models, supporting the development of parameterizations for improving the representation of marine secondary particle formation. Our findings further facilitate the interpretation of field data, clarify the chemical sources of these fresh particles, and offer valuable guidance for multi-component focus in future field measurements as well as analysis of the chemical composition of marine new particles.

In summary, this study's value extends beyond validating observations: it mechanistically explains the efficiency of NPF in marine environments by emphasizing multi-component synergy, strengthens our ability to predict these processes, and provides actionable insights for model development, field observations, and chemical composition analysis.

Reference:

Almeida, J., Schobesberger, S., Kürten, A., Ortega, I. K., Kupiainen-Määttä, O., Praplan, A. P., Adamov, A., Amorim, A., Bianchi, F., Breitenlechner, M., David, A., Dommen, J., Donahue, N. M., Downard, A., Dunne, E., Duplissy, J., Ehrhart, S., Flagan, R. C., Franchin, A., Guida, R., Hakala, J., Hansel, A., Heinritzi, M., Henschel, H., Jokinen, T., Junninen, H., Kajos, M., Kangasluoma, J., Keskinen, H., Kupc, A., Kurten, T., Kvashin, A. N., Laaksonen, A., Lehtipalo, K., Leiminger, M., Leppä, J., Loukonen, V., Makhmutov, V., Mathot, S., McGrath, M. J., Nieminen, T., Olenius, T., Onnela, A., Petäjä, T., Riccobono, F., Riipinen, I., Rissanen, M., Rondo, L., Ruuskanen, T., Santos, F. D., Sarnela, N., Schallhart, S., Schnitzhofer, R., Seinfeld, J. H., Simon, M., Sipilä, M., Stozhkov, Y., Stratmann, F., Tomé, A., Tröstl, J., Tsagkogeorgas, G., Vaattovaara, P., Viisanen, Y., Virtanen, A., Vrtala, A., Wagner, P. E., Weingartner, E., Wex, H., Williamson, C., Wimmer, D., Ye, P., Yli-Juuti, T., Carslaw, K. S., Kulmala, M., Curtius, J., Baltensperger, U., Worsnop, D. R., Vehkamäki, H. and Kirkby, J.: Molecular understanding of sulphuric acid-amine particle nucleation in the atmosphere, Nature, 502, 359–363, http://doi.org/10.1038/nature12663, 2013.

Berresheim, H., Elste, T., Rosman, K., Dal Maso, M., Tremmel, H. G., Mäkelä, J. M., Allen, A. G., Kulmala, M. and Hansson, H.-C.: Gas-aerosol relationships of H_2SO_4, MSA, and OH: Observations in the coastal marine boundary layer at Mace Head, Ireland, J. Geophys. Res.-Atmos., 107, PAR 5-1–PAR 5-12, http://doi.org/10.1029/2000jd000229, 2002.

Besel, V., Kubečka, J., Kurtén, T. and Vehkamäki, H.: Impact of Quantum Chemistry Parameter Choices and Cluster Distribution Model Settings on Modeled Atmospheric Particle Formation Rates, J. Phys. Chem. A, 124, 5931–5943, http://doi.org/10.1021/acs.jpca.0c03984, 2020.

Chen, J., Lane, J. R., Bates, K. H. and Kjaergaard, H. G.: Atmospheric Gas-Phase Formation of Methanesulfonic Acid, Environ. Sci. Technol., 57, 21168−21177, http://doi.org/10.1021/acs.est.3c07120, 2023.

Eisele, F. L. and Tanner, D. J.: Measurement of the gas phase concentration of H_2SO_4 and methane sulfonic acid and estimates of H_2SO_4 production and loss in the atmosphere, J. Geophys. Res., 98, 9001–9010, http://doi.org/10.1029/93JD00031, 1993.

Engsvang, M., Wu, H. and Elm, J.: Iodine clusters in the atmosphere I: Computational benchmark and dimer formation of oxyacids and oxides, ACS Omega, 9, 31521–31532, http://doi.org/10.1021/acsomega.4c01235, 2024.

Finkenzeller, H., Iyer, S., He, X. C., Simon, M., Koenig, T. K., Lee, C. F., Valiev, R., Hofbauer, V., Amorim, A., Baalbaki, R., Baccarini, A., Beck, L., Bell, D. M., Caudillo, L., Chen, D., Chiu, R., Chu, B., Dada, L., Duplissy, J., Heinritzi, M., Kemppainen, D., Kim, C., Krechmer, J., Kurten, A., Kvashnin, A., Lamkaddam, H., Lee, C. P., Lehtipalo, K., Li, Z., Makhmutov, V., Manninen, H. E., Marie, G., Marten, R., Mauldin, R. L., Mentler, B., Muller, T., Petaja, T., Philippov, M., Ranjithkumar, A., Rorup, B., Shen, J., Stolzenburg, D., Tauber, C., Tham, Y. J., Tome, A., Vazquez-Pufleau, M., Wagner, A. C., Wang, D. S., Wang, M., Wang, Y., Weber, S. K., Nie, W., Wu, Y., Xiao, M., Ye, Q., Zauner-Wieczorek, M., Hansel, A., Baltensperger, U., Brioude, J., Curtius, J., Donahue, N. M., Haddad, I. E., Flagan, R. C., Kulmala, M., Kirkby, J., Sipila, M., Worsnop, D. R., Kurten, T., Rissanen, M. and Volkamer, R.: The gas-phase formation mechanism of iodic acid as an atmospheric aerosol source, Nat. Commun., 15, 129–135, http://doi.org/10.1038/s41557-022-01067-z, 2023.

He, X.-C., Simon, M., Iyer, S., Xie, H.-B., Rörup, B., Shen, J., Finkenzeller, H., Stolzenburg, D., Zhang,

R., Baccarini, A., Tham, Y. J., Wang, M., Amanatidis, S., Piedehierro, A. A., Amorim, A., Baalbaki, R., Brasseur, Z., Caudillo, L., Chu, B., Dada, L., Duplissy, J., Haddad, I. E., Flagan, R. C., Granzin, M., Hansel, A., Heinritzi, M., Hofbauer, V., Jokinen, T., Kemppainen, D., Kong, W., Krechmer, J., Kürten, A., Lamkaddam, H., Lopez, B., Ma, F., Mahfouz, N. G. A., Makhmutov, V., Manninen, H. E., Marie, G., Marten, R., Massabò, D., Mauldin, R. L., Mentler, B., Onnela, A., Petäjä, T., Pfeifer, J., Philippov, M., Ranjithkumar, A., Rissanen, M. P., Schobesberger, S., Scholz, W., Schulze, B., Surdu, M., Thakur, R. C., Tomé, A., Wagner, A. C., Wang, D., Wang, Y., Weber, S. K., Welti, A., Winkler, P. M., Zauner-Wieczorek, M., Baltensperger, U., Curtius, J., Kurtén, T., Worsnop, D. R., Volkamer, R., Lehtipalo, K., Kirkby, J., Donahue, N. M., Sipilä, M. and Kulmala, M.: Iodine oxoacids enhance nucleation of sulfuric acid particles in the atmosphere, Science, 382, 1308–1314, http://doi.org/10.1126/science.adh2526, 2023.

He, X.-C., Tham, Y. J., Dada, L., Wang, M., Finkenzeller, H., Stolzenburg, D., Iyer, S., Simon, M., ¨rten, A. K., Shen, J., Roerup, B., Rissanen, M., Schobesberger, S., Baalbaki, R., Wang, D. S., Koenig, T. K., Jokinen, T., Sarnela, N., Beck, L. J., Almeida, J., Amanatidis, S., Amorim, A., Ataei, F., Baccarini, A., Bertozzi, B., Bianchi, F., Brilke, S., Caudillo, L., Chen, D., Chiu, R., Chu, B., Dias, A., Ding, A., Dommen, J., Duplissy, J., Haddad, I. E., Carracedo, L. G., Granzin, M., Hansel, A., Heinritzi, M., Hofbauer, V., Junninen, H., Kangasluoma, J., Kemppainen, D., Kim, C., Kong, W., Krechmer, J. E., Kvashin, A., Laitinen, T., Lamkaddam, H., Lee, C. P., Lehtipalo, K., Leiminger, M., Li, Z., Makhmutov, V., Manninen, H. E., Marie, G., Marten, R., Mathot, S., Mauldin, R. L., Mentler, B., Moehler, O., Mueller, T., Nie, W., Onnela, A., Petaja, T., Pfeifer, J., Philippov, M., Ranjithkumar, A., Saiz-Lopez, A., Salma, I., Scholz, W., Schuchmann, S., Schulze, B., Steiner, G., Stozhkov, Y., Tauber, C., Tome, A., Thakur, R. C., Vaisanen, O., Vazquez-Pufleau, M., Wagner, A. C., Wang, Y., Weber, S. K., Winkler, P. M., Wu, Y., Xiao, M., Yan, C., Ye, Q., Ylisirnio, A., Zauner-Wieczorek, M., Zha, Q., Zhou, P., Flagan, R. C., Curtius, J., Baltensperger, U., Kulmala, M., Kerminen, V.-M., Kurten, T., Donahue, N. M., Volkamer, R., Kirkby, J., Worsnop, D. R. and Sipila, M.: Role of iodine oxoacids in atmospheric aerosol nucleation, Science, 371, 589–595, http://doi.org/10.1126/science.abe0298, 2021.

Jokinen, T., Sipilä, M., Kontkanen, J., Vakkari, V., Tisler, P., Duplissy, E.-M., Junninen, H., Kangasluoma, J., Manninen, H. E., Petäjä, T., Kulmala, M., Worsnop, D. R., Kirkby, J., Virkkula, A. and Kerminen, V.-M.: Ion-induced sulfuric acid–ammonia nucleation drives particle formation in coastal Antarctica, Sci. Adv., 4, eaat9744, http://doi.org/10.1126/sciadv.aat9744, 2018.

Khanniche, S., Louis, F., Cantrel, L. and Černušák, I.: A theoretical study of the microhydration of iodic acid (HOIO2), Comput. Theor. Chem., 1094, 98-107, http://doi.org/10.1016/j.comptc.2016.09.010, 2016.

Khanniche, S., Louis, F., Cantrel, L. and Černušák, I.: Thermochemistry of HIO2 Species and Reactivity of Iodous Acid with OH Radical: A Computational Study, ACS Earth Space Chem., 1, 39-49, http://doi.org/10.1021/acsearthspacechem.6b00010, 2017.

Kubečka, J., Neefjes, I., Besel, V., Qiao, F., Xie, H.-B. and Elm, J.: Atmospheric Sulfuric Acid-Multi-Base New Particle Formation Revealed through Quantum Chemistry Enhanced by Machine Learning, J. Phys. Chem. A, 127, 2091–2103, http://doi.org/10.1021/acs.jpca.3c00068, 2023.

Kulmala, M., Kontkanen, J., Junninen, H., Lehtipalo, K., Manninen, H. E., Nieminen, T., Petäjä, T., Sipilä, M., Schobesberger, S., Rantala, P., Franchin, A., Jokinen, T., Järvinen, E., Äijälä, M., Kangasluoma, J., Hakala, J., Aalto, P. P., Paasonen, P., Mikkilä, J., Vanhanen, J., Aalto, J., Hakola, H., Makkonen,

U., Ruuskanen, T., Mauldin, R. L., 3rd, Duplissy, J., Vehkamäki, H., Bäck, J., Kortelainen, A., Riipinen, I., Kurtén, T., Johnston, M. V., Smith, J. N., Ehn, M., Mentel, T. F., Lehtinen, K. E., Laaksonen, A., Kerminen, V. M. and Worsnop, D. R.: Direct observations of atmospheric aerosol nucleation, Science, 339, 943–946, http://doi.org/10.1126/science.1227385, 2013.

Liakos, D. G., Guo, Y. and Neese, F.: Comprehensive Benchmark Results for the Domain Based Local Pair Natural Orbital Coupled Cluster Method (DLPNO-CCSD(T)) for Closed- and Open-Shell Systems, J. Phys. Chem. A, 124, 90–100, http://doi.org/10.1021/acs.jpca.9b05734, 2020.

Liu, L., Li, S., Zu, H. and Zhang, X.: Unexpectedly significant stabilizing mechanism of iodous acid on iodic acid nucleation under different atmospheric conditions, Sci. Total Environ., 859, 159832, http://doi.org/10.1016/j.scitotenv.2022.159832, 2023.

Ma, F., Xie, H. B., Zhang, R., Su, L., Jiang, Q., Tang, W., Chen, J., Engsvang, M., Elm, J. and He, X. C.: Enhancement of atmospheric nucleation precursors on iodic acid-induced nucleation: Predictive model and mechanism, Environ. Sci. Technol., 57, 6944–6954, http://doi.org/10.1021/acs.est.3c01034, 2023.

Myllys, N., Kubečka, J., Besel, V., Alfaouri, D., Olenius, T., Smith, J. N. and Passananti, M.: Role of base strength, cluster structure and charge in sulfuric-acid-driven particle formation, Atmos. Chem. Phys., 19, 9753–9768, http://doi.org/10.5194/acp-19-9753-2019, 2019.

Ning, A., Liu, L., Zhang, S., Yu, F., Du, L., Ge, M. and Zhang, X.: The critical role of dimethylamine in the rapid formation of iodic acid particles in marine areas, npj Clim. Atmos. Sci., 5, 92, http://doi.org/10.1038/s41612-022-00316-9, 2022.

Quéléver, L. L. J., Dada, L., Asmi, E., Lampilahti, J., Chan, T., Ferrara, J. E., Copes, G. E., Pérez-Fogwill, G., Barreira, L., Aurela, M., Worsnop, D. R., Jokinen, T. and Sipilä, M.: Investigation of new particle formation mechanisms and aerosol processes at Marambio Station, Antarctic Peninsula, Atmos. Chem. Phys., 22, 8417–8437, http://doi.org/10.5194/acp-22-8417-2022, 2022.

Salignat, R., Rissanen, M., Iyer, S., Baray, J.-L., Tulet, P., Metzger, J.-M., Brioude, J., Sellegri, K. and Rose, C.: Measurement report: Insights into the chemical composition and origin of molecular clusters and potential precursor molecules present in the free troposphere over the southern Indian Ocean: observations from the Maïdo Observatory (2150 m a.s.l., Réunion), Atmos. Chem. Phys., 24, 3785–3812, http://doi.org/10.5194/acp-24-3785-2024, 2024.

Scholz, W., Shen, J., Aliaga, D., Wu, C., Carbone, S., Moreno, I., Zha, Q., Huang, W., Heikkinen, L., Jaffrezo, J. L., Uzu, G., Partoll, E., Leiminger, M., Velarde, F., Laj, P., Ginot, P., Artaxo, P., Wiedensohler, A., Kulmala, M., Mohr, C., Andrade, M., Sinclair, V., Bianchi, F. and Hansel, A.: Measurement report: Long-range transport and the fate of dimethyl sulfide oxidation products in the free troposphere derived from observations at the high-altitude research station Chacaltaya (5240 m a.s.l.) in the Bolivian Andes, Atmos. Chem. Phys., 23, 895–920, http://doi.org/10.5194/acp-23-895-2023, 2023.

Takashima, H., Kanaya, Y., Kato, S., Friedrich, M. M., Van Roozendael, M., Taketani, F., Miyakawa, T., Komazaki, Y., Cuevas, C. A., Saiz-Lopez, A. and Sekiya, T.: Full latitudinal marine atmospheric measurements of iodine monoxide, Atmos. Chem. Phys., 22, 4005–4018, http://doi.org/10.5194/acp-22-4005-2022, 2022.

Xavier, C., de Jonge, R. W., Jokinen, T., Beck, L., Sipila, M., Olenius, T. and Roldin, P.: Role of Iodine-Assisted Aerosol Particle Formation in Antarctica, Environ. Sci. Technol., 58, 7314–7324, http://doi.org/10.1021/acs.est.3c09103, 2024.

Xia, D., Chen, J., Yu, H., Xie, H. B., Wang, Y., Wang, Z., Xu, T. and Allen, D. T.: Formation Mechanisms of Iodine-Ammonia Clusters in Polluted Coastal Areas Unveiled by Thermodynamics and Kinetic Simulations, Environ. Sci. Technol., 54, 9235–9242, http://doi.org/10.1021/acs.est.9b07476, 2020.

Yan, J., Jung, J., Zhang, M., Xu, S., Lin, Q., Zhao, S. and Chen, L.: Significant Underestimation of Gaseous Methanesulfonic Acid (MSA) over Southern Ocean, Environ. Sci. Technol., 53, 13064–13070, http://doi.org/10.1021/acs.est.9b05362, 2019.

Zhang, R., Xie, H. B., Ma, F., Chen, J., Iyer, S., Simon, M., Heinritzi, M., Shen, J., Tham, Y. J., Kurtén, T., Worsnop, D. R., Kirkby, J., Curtius, J., Sipilä, M., Kulmala, M. and He, X. C.: Critical Role of Iodous Acid in Neutral Iodine Oxoacid Nucleation, Environ. Sci. Technol., 56, 14166–14177, http://doi.org/10.1021/acs.est.2c04328, 2022.

Zhou, S., Chen, Y., Paytan, A., Li, H., Wang, F., Zhu, Y., Yang, T., Zhang, Y. and Zhang, R.: Non-Marine Sources Contribute to Aerosol Methanesulfonate Over Coastal Seas, J. Geophys. Res.-Atmos., 126, http://doi.org/10.1029/2021jd034960, 2021.